

Photons production in heavy ion collisions as a signal of deconfinement phase

Sergei Nedelko* and Aleksei Nikolskii†

Bogoliubov Laboratory of Theoretical Physics, JINR, 141980 Dubna, Russia

arXiv:2208.00842v1 [hep-ph] 1 Aug 2022

Abstract

The production of photons in the process of gluon conversion $gg \rightarrow \gamma$ in the presence of background gauge fields is studied within the mean-field approach to QCD vacuum, the domain model of QCD vacuum and hadronization. In this approach, Abelian (anti-)self-dual gluon mean field dominates the confinement phase while the deconfined phase can be characterized by the strong chromomagnetic fields. It is shown that, due to the randomness of the vacuum mean fields, the probability of conversion of two gluons into photon vanishes in confinement phase. In contrast, a strong electromagnetic field, generated in the collision processes of relativistic heavy ions, serves as a catalyst for deconfinement with the appearance of mean chromomagnetic field that is singled out in the spacial direction, which leads to nonzero probability of the conversion of two gluons into a photon. The angular distribution of the generated photons is expected to be strongly anisotropic.

I. INTRODUCTION

Extremely strong electromagnetic fields generated during the collisions of relativistic heavy ions [1, 2] may lead to numerous physical effects [3–7]. The generated magnetic field has a preferable space direction which is manifested through the angular anisotropies in various observables. Besides the direct effects of quark field interaction with the electromagnetic field there can be even more vigorous effects related to a kind of polarization of the QCD vacuum caused by the effective interaction of gluon and electromagnetic fields via their coupling to the quark fields, which are known to play the catalyzing role for deconfinement [8–14]. A plausible interpretation of the mechanism of the catalysis was offered within the mean field approach to nonperturbative QCD vacuum [8, 9, 15]. The main observation of these papers is that in the presence of external magnetic field there exists a global minimum of the one-loop quark contribution to the effective potential of QCD corresponding to purely chromomagnetic ($F_{\mu\nu}^a \tilde{F}_{\mu\nu}^a = 0$) gluon field. In contrast to the Abelian (anti-)self-dual homogeneous gluon field, which is a plausible candidate for a global minimum of the effective QCD potential in the absence of external electromagnetic fields (e.g., see [16, 17]), the chromomagnetic gluon field does not support confinement, since the color charged quasi-

* nedelko@theor.jinr.ru

† alexn@theor.jinr.ru

particles do exist and can move along the direction of the chromomagnetic field, which in turn coincides with the direction of magnetic field [9]. Such an interpretation appears to be consistent with the lattice QCD studies [10, 11, 18].

It should be noted that according to the mean field interpretation an anisotropic background chromomagnetic field can exist as long as the deconfinement phase occurs, unlike the short-lived extreme magnetic field which simply triggers the anisotropy (for details see [9]). The presence of the chromomagnetic background gauge fields violates the conditions of the Furry theorem, and thus leads to the possibility of conversion of a pair of gluons into photon through the quark loop, which can be seen as an important mechanism for the generation of direct photons in the deconfinement phase, similarly to the case of magnetic background discussed in papers [6, 19–22].

In experiments of ALICE and PHENIX collaborations an abnormally high photon yields and degree of azimuthal anisotropy were observed [23–25]. This effect is known as direct photon flow puzzle. Various phenomenological explanations of this phenomenon were proposed over the years [3, 26–35], including the mechanism based on Furry theorem violation by the electromagnetic fields generated during the heavy ion collisions [6, 19]

Due to its long-lived nature and high field strength, defined as a matter of fact by the value of the scalar gluon condensate $\langle g^2 F^2 \rangle$, the chromomagnetic background has clearly promising potential for explaining both puzzling features of direct photon measurements, spectra and anisotropy, simultaneously.

In this paper we calculate the contribution of the quark loop shown in Fig.1 to the process $gg \rightarrow \gamma$ for two regimes: in the presence of confining vacuum mean field, represented by the statistical ensemble of the almost everywhere homogeneous (anti-)self-dual Abelian gluon fields, and for the case of anisotropic chromomagnetic field characteristic of the deconfinement regime. In the confinement phase, due to the random nature of the mean field, this contribution vanishes on average. In deconfinement regime the direction of the chromomagnetic field is correlated with the direction of the short-lived generated magnetic field, the conditions of the Furry theorem are thus violated, and the diagram in Fig.1 gives a nonzero contribution. The estimate elaborated in line with papers [6, 19] indicates rather strong effect of conversion of gluons to photon in deconfinement phase. The appearance of an additional photon source due to the process $gg \rightarrow \gamma$ may be seen as a signal for deconfinement.

Studies of the present paper have to be considered in the context of the domain model of QCD vacuum and hadronization [8, 9, 16, 17, 36, 37]. The model is based on the vacuum mean field represented by the ensemble of domain-structured configurations of almost everywhere homogeneous Abelian (anti-)self-dual gluon field which is treated nonperturbatively. This mean-field provides simultaneously confinement of static and dynamic quarks - the area law for the Wilson loop and the absence of poles in the quark propagator in the complex momentum plane respectively, as well as flavour chiral symmetry breaking and the resolution of the $U_A(1)$ problem. Upon bosonization, this mean field approach successfully describes the masses of light, heavy-light mesons and heavy quarkonia, including their excited states, as well as the decay constants and form factors. The mean field does not affect the UV-behaviour of quark, gluon and ghost propagators, but otherwise strongly modifies the propagators, whose form is overall consistent with the results of the functional renormalization group and lattice QCD (for complete analysis see [36]).

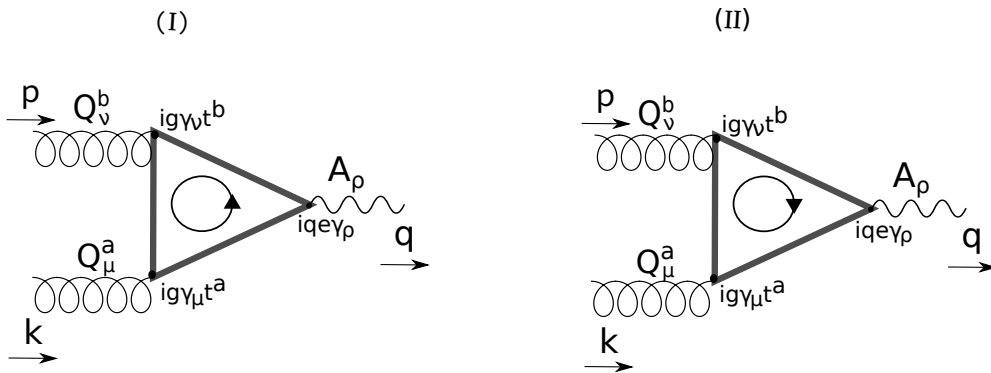


FIG. 1. The diagrams of process $gg \rightarrow \gamma$ in the presence of homogeneous Abelian gauge field. p, k - is the gluons momenta, q is the photon momentum. The arrows inside loop indicate the direction of loop momentum.

II. THE CONFINEMENT PHASE

In this section, we consider the amplitude for the process $gg \rightarrow \gamma$ *via* quark loop (Fig.1) in the presence of a random ensemble of almost everywhere homogeneous Abelian (anti-

)self-dual gluon field:

$$\begin{aligned}
\hat{B}_\mu &= \frac{1}{2}\hat{B}_{\mu\nu}x_\nu, \quad \hat{B}_{\mu\nu} = \hat{n}B_{\mu\nu}, \quad \hat{n} = t^8, \\
\tilde{B}_{\mu\nu} &= \frac{1}{2}\epsilon_{\mu\nu\alpha\beta}B_{\alpha\beta} = \pm B_{\mu\nu}, \quad \hat{B}_{\rho\mu}\hat{B}_{\rho\nu} = 4v^2B^2\delta_{\mu\nu}, \\
\hat{f}_{\alpha\beta} &= \frac{\hat{n}}{2vB}B_{\alpha\beta}, \quad v = \text{diag}\left(\frac{1}{6}, \frac{1}{6}, \frac{1}{3}\right), \quad \hat{f}_{\mu\alpha}\hat{f}_{\nu\alpha} = \delta^{ij}\delta_{\mu\nu},
\end{aligned} \tag{1}$$

where field strength B sets the scale related to the value of the scalar gluon condensate.

The propagator of the quark field with mass m_f in the presence of the field (1) has the form [36]

$$\begin{aligned}
S_f(x, y) &= \exp\left(\frac{i}{2}x_\mu\hat{B}_{\mu\nu}y_\nu\right) H_f(x - y), \\
H_f(z) &= \frac{vB}{8\pi^2} \int_0^1 \frac{ds}{s^2} \exp\left(-\frac{vB}{2s}z^2\right) \left(\frac{1-s}{1+s}\right)^{\frac{m_f^2}{4vB}} \\
&\quad \times \left[-i\frac{vB}{s}z_\mu\left(\gamma_\mu \pm is\hat{f}_{\mu\nu}\gamma_\nu\gamma_5\right) + m_f\left(P_\pm + \frac{1+s^2}{1-s^2}P_\mp + \frac{i}{2}\gamma_\mu\hat{f}_{\mu\nu}\gamma_\nu\frac{s}{1-s^2}\right)\right],
\end{aligned} \tag{2}$$

where anti-Hermitian representation of Dirac matrices in Euclidean space-time is used. Sign ” \pm ” corresponds to (anti-)self-duality of the background field (1). The Fourier transform of translation invariant part H_f of the propagator is an entire analytical function in the complex momentum plane. It approaches the limit of the standard free Dirac propagator at large Euclidean momentum $p^2 \gg B$.

The amplitudes for diagrams (I) and (II) in Fig.1 take the form

$$\begin{aligned}
M^{(I)} &= ieg^2 \int d^4x d^4y d^4z e^{-i(px+ky-qz)} \langle \text{Tr} [\gamma_\nu t^b S(x, z) Q \gamma_\rho S(z, y) \gamma_\mu t^a S(y, x)] \rangle \epsilon_\mu^a(k) \epsilon_\nu^b(p) \epsilon_\rho(q), \\
M^{(II)} &= ieg^2 \int d^4x d^4y d^4z e^{-i(px+ky-qz)} \langle \text{Tr} [S(x, y) \gamma_\mu t^a S(y, z) Q \gamma_\rho S(z, x) \gamma_\nu t^b] \rangle \epsilon_\mu^a(k) \epsilon_\nu^b(p) \epsilon_\rho(q),
\end{aligned}$$

where g is the strong coupling constant, e is the electron charge, Q is a diagonal matrix of the fractions of electric charges of quarks with flavor f , vectors ϵ define the polarization of the gluons and photon. Tr denotes trace of the color, Dirac and flavor matrices, and $\langle \dots \rangle$ denotes averaging of the amplitude over different random configurations of the background confining field - (anti-)self-duality and spacial orientation. In particular, integration over

spacial orientations of the background field is given by the master formula [37]

$$\langle \exp(i f_{\mu\nu} J_{\mu\nu}) \rangle = \frac{\sin \sqrt{2 \left(J_{\mu\nu} J_{\mu\nu} \pm J_{\mu\nu} \tilde{J}_{\mu\nu} \right)}}{\sqrt{2 \left(J_{\mu\nu} J_{\mu\nu} \pm J_{\mu\nu} \tilde{J}_{\mu\nu} \right)}}, \quad (3)$$

where $J_{\mu\nu}$ is an arbitrary antisymmetric tensor.

Taking into account Eq.(2) one may integrate over one of the spacial coordinates and arrive at the representation

$$M^{(I)} = i e g^2 (2\pi)^4 \delta^{(4)}(p+k-q) \int d^4 x d^4 y e^{-i(px+ky)} \\ \times \left\langle \text{Tr} \left[e^{-ivBy^\mu \hat{f}_{\mu\nu} x^\nu} \gamma_\nu t^b H(x) Q \gamma_\rho H(-y) \gamma_\mu t^a H(y-x) \right] \right\rangle \epsilon_\mu^a(k) \epsilon_\nu^b(p) \epsilon_\rho(q), \quad (4)$$

$$M^{(II)} = i e g^2 (2\pi)^4 \delta^{(4)}(p+k-q) \int d^4 x d^4 y e^{-i(px+ky)} \\ \times \left\langle \text{Tr} \left[e^{-ivBx^\mu \hat{f}_{\mu\nu} y^\nu} H(x-y) \gamma_\mu t^a H(y) Q \gamma_\rho H(-x) \gamma_\nu t^b \right] \right\rangle \epsilon_\mu^a(k) \epsilon_\nu^b(p) \epsilon_\rho(q), \quad (5)$$

The terms in the amplitudes $M^{(I)}$ and $M^{(II)}$ with odd powers of field strength tensor $\hat{f}_{\mu\nu}$ violate the conditions of the Furry theorem. It becomes explicit by substitution of quark propagator $H_f(z)$ in (4) and (5) resulting in the following representation

$$M^{(I)} = i e g^2 q_f (2\pi)^4 \delta^{(4)}(p+k-q) \left(\frac{vB}{8\pi^2} \right)^3 \int_0^1 \int_0^1 \int_0^1 \frac{ds_1}{s_1^2} \frac{ds_2}{s_2^2} \frac{ds_3}{s_3^2} \frac{(-ivB)^3}{s_1 s_2 s_3} \\ \left(\frac{1-s_1}{1+s_1} \right)^{\frac{m_f^2}{4vB}} \left(\frac{1-s_2}{1+s_2} \right)^{\frac{m_f^2}{4vB}} \left(\frac{1-s_3}{1+s_3} \right)^{\frac{m_f^2}{4vB}} \int d^4 x d^4 y e^{-i(px+ky)} \\ \times \left\langle \text{Tr} \left[e^{-ivBy^\mu \hat{f}_{\mu\nu} x^\nu - \frac{v}{2s_1} x^2 - \frac{v}{2s_2} y^2 - \frac{v}{2s_3} (y-x)^2} \right. \right. \\ \hat{f}_{\alpha\omega} \hat{f}_{\beta\chi} \hat{f}_{\lambda\eta} (\pm s_1 s_2 s_3 x_\alpha x_\beta y_\lambda \gamma_5 \gamma_\nu \gamma_\omega \gamma_\rho \gamma_\eta \gamma_\mu \gamma_\chi \mp s_1 s_2 s_3 x_\alpha y_\beta y_\lambda \gamma_5 \gamma_\nu \gamma_\omega \gamma_\rho \gamma_\eta \gamma_\mu \gamma_\chi) \\ \hat{f}_{\alpha\eta} \hat{f}_{\beta\omega} (-i s_2 s_3 x_\alpha y_\beta x_\lambda \gamma_\nu \gamma_\lambda \gamma_\rho \gamma_\omega \gamma_\mu \gamma_\eta + i s_2 s_3 y_\alpha y_\beta x_\lambda \gamma_\nu \gamma_\lambda \gamma_\rho \gamma_\omega \gamma_\mu \gamma_\eta \\ - i s_1 s_3 x_\alpha y_\beta x_\lambda \gamma_\nu \gamma_\omega \gamma_\rho \gamma_\lambda \gamma_\mu \gamma_\eta + i s_1 s_3 x_\alpha y_\beta x_\lambda \gamma_\nu \gamma_\omega \gamma_\rho \gamma_\beta \gamma_\mu \gamma_\eta \\ - i s_1 s_2 x_\alpha y_\beta x_\lambda \gamma_\nu \gamma_\omega \gamma_\rho \gamma_\eta \gamma_\mu \gamma_\alpha + i s_1 s_2 y_\alpha y_\beta x_\lambda \gamma_\nu \gamma_\omega \gamma_\rho \gamma_\eta \gamma_\mu \gamma_\alpha) \\ \left. \hat{f}_{\alpha\omega} (\mp s_3 x_\alpha x_\beta y_\lambda \gamma_5 \gamma_\nu \gamma_\beta \gamma_\rho \gamma_\lambda \gamma_\mu \gamma_\omega \pm s_3 y_\alpha x_\beta y_\lambda \gamma_5 \gamma_\nu \gamma_\beta \gamma_\rho \gamma_\lambda \gamma_\mu \gamma_\omega \mp s_2 y_\alpha x_\beta x_\lambda \gamma_5 \gamma_\nu \gamma_\beta \gamma_\rho \gamma_\omega \gamma_\mu \gamma_\lambda \right. \\ \left. \pm s_2 y_\alpha x_\beta y_\lambda \gamma_5 \gamma_\nu \gamma_\beta \gamma_\rho \gamma_\omega \gamma_\mu \gamma_\lambda \mp s_1 x_\alpha y_\beta x_\lambda \gamma_5 \gamma_\nu \gamma_\omega \gamma_\rho \gamma_\beta \gamma_\mu \gamma_\lambda \pm s_1 x_\alpha y_\beta y_\lambda \gamma_5 \gamma_\nu \gamma_\omega \gamma_\rho \gamma_\beta \gamma_\mu \gamma_\lambda) \right. \\ \left. + i x_\alpha y_\beta x_\lambda \gamma_\nu \gamma_\alpha \gamma_\rho \gamma_\beta \gamma_\lambda - i x_\alpha y_\beta y_\lambda \gamma_\nu \gamma_\alpha \gamma_\rho \gamma_\beta \gamma_\lambda \right] \right\rangle \epsilon_\mu^a(k) \epsilon_\nu^b(p) \epsilon_\rho(q),$$

$$\begin{aligned}
M^{(II)} = & ieg^2 q_f (2\pi)^4 \delta^{(4)}(p+k-q) \left(\frac{vB}{8\pi^2}\right)^3 \int_0^1 \int_0^1 \int_0^1 \frac{ds_1}{s_1^2} \frac{ds_2}{s_2^2} \frac{ds_3}{s_3^2} \frac{(-ivB)^3}{s_1 s_2 s_3} \\
& \left(\frac{1-s_1}{1+s_1}\right)^{\frac{m_f^2}{4vB}} \left(\frac{1-s_2}{1+s_2}\right)^{\frac{m_f^2}{4vB}} \left(\frac{1-s_3}{1+s_3}\right)^{\frac{m_f^2}{4vB}} \int d^4x d^4y e^{-i(px+ky)} \\
& \times \left\langle \text{Tr} \left[e^{-ivBx^\mu \hat{f}_{\mu\nu} y^\nu - \frac{v}{2s_1}(x-y)^2 - \frac{v}{2s_2}y^2 - \frac{v}{2s_3}x^2} \right. \right. \\
& \hat{f}_{\alpha\omega} \hat{f}_{\beta\chi} \hat{f}_{\lambda\eta} (\pm s_1 s_2 s_3 x_\alpha x_\beta y_\lambda \gamma_5 \gamma_\nu \gamma_\omega \gamma_\rho \gamma_\eta \gamma_\mu \gamma_\chi \mp s_1 s_2 s_3 x_\alpha y_\beta y_\lambda \gamma_5 \gamma_\nu \gamma_\omega \gamma_\rho \gamma_\eta \gamma_\mu \gamma_\chi) \\
& - \hat{f}_{\alpha\eta} \hat{f}_{\beta\omega} (-is_2 s_3 x_\alpha y_\beta x_\lambda \gamma_\nu \gamma_\lambda \gamma_\rho \gamma_\omega \gamma_\mu \gamma_\eta + is_2 s_3 y_\alpha y_\beta x_\lambda \gamma_\nu \gamma_\lambda \gamma_\rho \gamma_\omega \gamma_\mu \gamma_\eta \\
& - is_1 s_3 x_\alpha y_\beta x_\lambda \gamma_\nu \gamma_\omega \gamma_\rho \gamma_\lambda \gamma_\mu \gamma_\eta + is_1 s_3 x_\alpha y_\beta x_\lambda \gamma_\nu \gamma_\omega \gamma_\rho \gamma_\beta \gamma_\mu \gamma_\eta \\
& - is_1 s_2 x_\alpha y_\beta x_\lambda \gamma_\nu \gamma_\omega \gamma_\rho \gamma_\eta \gamma_\mu \gamma_\alpha + is_1 s_2 y_\alpha y_\beta x_\lambda \gamma_\nu \gamma_\omega \gamma_\rho \gamma_\eta \gamma_\mu \gamma_\alpha) \\
& \left. \hat{f}_{\alpha\omega} (\mp s_3 x_\alpha x_\beta y_\lambda \gamma_5 \gamma_\nu \gamma_\beta \gamma_\rho \gamma_\lambda \gamma_\mu \gamma_\omega \pm s_3 y_\alpha x_\beta y_\lambda \gamma_5 \gamma_\nu \gamma_\beta \gamma_\rho \gamma_\lambda \gamma_\mu \gamma_\omega \mp s_2 y_\alpha x_\beta x_\lambda \gamma_5 \gamma_\nu \gamma_\beta \gamma_\rho \gamma_\omega \gamma_\mu \gamma_\lambda \right. \\
& \left. \pm s_2 y_\alpha x_\beta y_\lambda \gamma_5 \gamma_\nu \gamma_\beta \gamma_\rho \gamma_\omega \gamma_\mu \gamma_\lambda \mp s_1 x_\alpha y_\beta x_\lambda \gamma_5 \gamma_\nu \gamma_\omega \gamma_\rho \gamma_\beta \gamma_\mu \gamma_\lambda \pm s_1 x_\alpha y_\beta y_\lambda \gamma_5 \gamma_\nu \gamma_\omega \gamma_\rho \gamma_\beta \gamma_\mu \gamma_\lambda) \right. \\
& \left. - ix_\alpha y_\beta x_\lambda \gamma_\nu \gamma_\alpha \gamma_\rho \gamma_\beta \gamma_\lambda + ix_\alpha y_\beta y_\lambda \gamma_\nu \gamma_\alpha \gamma_\rho \gamma_\beta \gamma_\lambda \right] \rangle \epsilon_\mu^a(k) \epsilon_\nu^b(p) \epsilon_\rho(q),
\end{aligned}$$

where q_f is the ratio of quark electric charge to the electron charge. The terms with the product of an even number of tensor $\hat{f}_{\mu\nu}$ in $M^{(I)}$ and $M^{(II)}$ have opposite signs, while the signs in front of the terms with an odd number of $\hat{f}_{\mu\nu}$ coincide. In addition, the amplitudes $M^{(I)}$ and $M^{(II)}$ differ by the sign of the phase factor: $e^{i\hat{f}_{\mu\nu}J_{\mu\nu}}$ for diagram (I) and $e^{-i\hat{f}_{\mu\nu}J_{\mu\nu}}$ for diagram (II). The sign of the phase factor is reflected in the result of averaging over the spacial orientation of the background field (for details see [37])

$$\left\langle \prod_{j=1}^n f_{\alpha_j \beta_j} e^{\pm i f_{\mu\nu} J_{\mu\nu}} \right\rangle = \frac{(\pm 1)^n}{(2i)^n} \prod_{j=1}^n \frac{\partial}{\partial J_{\alpha_j \beta_j}} \frac{\sin \sqrt{2 \left(J_{\mu\nu} J_{\mu\nu} \pm J_{\mu\nu} \tilde{J}_{\mu\nu} \right)}}{\sqrt{2 \left(J_{\mu\nu} J_{\mu\nu} \pm J_{\mu\nu} \tilde{J}_{\mu\nu} \right)}}, \quad (6)$$

and

$$\left\langle \prod_{j=1}^n f_{\alpha_j \beta_j} e^{-i f_{\mu\nu} J_{\mu\nu}} \right\rangle = (-1)^n \left\langle \prod_{j=1}^n f_{\alpha_j \beta_j} e^{i f_{\mu\nu} J_{\mu\nu}} \right\rangle. \quad (7)$$

Thus, the terms in $M^{(I)}$ and $M^{(II)}$ with the product of an even number of the field tensor $\hat{f}_{\mu\nu}$ cancel each other out identically just as in the case of the "usual" Furry theorem, and the terms with the product of an odd number of the field strength tensor cancel each other upon averaging. The amplitude $M = M^{(I)} + M^{(II)}$ vanishes in the confinement phase where averaging over random ensemble of almost everywhere homogeneous (anti-)self-dual

vacuum gluon fields must be applied. Conversion of two gluons to photon does not occur in the presence of the random ensemble of confining vacuum fields.

III. CHROMOMAGNETIC GLUON FIELDS AND PHOTON PRODUCTION IN DECONFINED PHASE

Within the mean field approach to QCD vacuum [8, 9] and the lattice QCD studies [10, 11] it has been indicated that the strong magnetic field generated in relativistic heavy ion collisions can play the role of a trigger for deconfinement transition to the phase characterized by the anisotropic chromomagnetic field. The chromomagnetic field exists as long as the deconfined phase persists, much longer than the initial pulse of the electromagnetic field. This is consistent with the indications that in the deconfining phase the scalar gluon condensate $\langle F^2 \rangle$ remains nonzero above the critical temperature while the mean absolute value of the topological charge density (or, equivalently, the condensate $\langle (F\tilde{F})^2 \rangle$) turns to zero. A relevance of nonzero absolute value of topological charge density to confinement has been discussed in lattice QCD (e.g., see [38–42]). Bearing this in mind it makes sense to estimate the magnitude of the photon generation effect due to the gluon conversion in the background constant homogeneous chromomagnetic field, which models the limiting case of the maximum anisotropy in the system.

As it has already been mentioned, the emergent long-lived chromomagnetic field and initially generated magnetic field are expected to be parallel to each other. It is convenient to select the third spacial axis x_3 along the direction of the background (chromo)magnetic field:

$$\hat{B}_{\mu\nu} = \hat{n}B_{\mu\nu} = \hat{n}Bf_{\mu\nu}, \quad f_{12} = -f_{21} = 1,$$

all other components of $f_{\mu\nu}$ are equal to zero. Respectively, it is convenient to denote:

$$x_{\perp} = (x_1, x_2, 0, 0), \quad x_{\parallel} = (0, 0, x_3, x_4).$$

The color charged quasi-particles with "masses" μ_n defined by the Landau levels can freely move along the chromomagnetic field and are confined in the transverse direction. Respectively, it is convenient to introduce notation for longitudinal p_{\parallel} and transverse p_{\perp} momenta

(in Euclidean space-time):

$$p_{\perp} = (p_1, p_2, 0, 0), \quad p_{\parallel} = (0, 0, p_3, p_4).$$

Complete, i.e. accounting for contribution of all Landau levels, propagator of the quark field with mass m_f in the presence of an external chromomagnetic field takes the form

$$S(x, y) = \exp \left\{ -\frac{i}{2} x_{\perp}^{\mu} \hat{B}_{\mu\nu} y_{\perp}^{\nu} \right\} H_f(x - y), \quad (8)$$

$$H_f(z) = \frac{B|\hat{n}|}{16\pi^2} \int_0^{\infty} \frac{ds}{s} [\coth(B|\hat{n}|s) - \sigma_{\rho\lambda} f_{\rho\lambda}] \exp \left\{ -m_f^2 s - \frac{1}{4s} z_{\parallel}^2 - \frac{1}{8s} [B|\hat{n}|s \coth(B|\hat{n}|s) + 1] z_{\perp}^2 \right\} \\ \left\{ m_f - \frac{i}{2s} \gamma_{\mu} z_{\parallel}^{\mu} - \frac{1}{2} \gamma_{\mu} \hat{B}_{\mu\nu} z_{\perp}^{\nu} - \frac{i}{4s} [B|\hat{n}|s \coth(B|\hat{n}|s) + 1] \gamma_{\mu} z_{\perp}^{\mu} \right\}, \\ \sigma_{\rho\lambda} = \frac{i}{2} [\gamma_{\rho}, \gamma_{\lambda}].$$

The amplitudes corresponding to diagrams (I) and (II) in Fig.1 take the form

$$M^{(I)} = i(2\pi)^4 \delta^{(4)}(p + k - q) g^2 e \sum_f q_f \int d^4 x d^4 y e^{-i(px+ky) - \frac{i}{2} \hat{n} B y_{\perp}^{\mu} f_{\mu\nu} x_{\perp}^{\nu}} \\ \times \text{Tr} [\gamma_{\nu} t^b H_f(x) Q \gamma_{\rho} H_f(-y) \gamma_{\mu} t^a H_f(y - x)] \epsilon_{\mu}^a(k) \epsilon_{\nu}^b(p) \epsilon_{\rho}(q), \quad (9)$$

$$M^{(II)} = i(2\pi)^4 \delta^{(4)}(p + k - q) g^2 e \sum_f q_f \int d^4 x d^4 y e^{-i(px+ky) - \frac{i}{2} \hat{n} B x_{\perp}^{\mu} f_{\mu\nu} y_{\perp}^{\nu}} \\ \times \text{Tr} [H_f(x - y) \gamma_{\mu} t^a H_f(y) Q \gamma_{\rho} H_f(-x) \gamma_{\nu} t^b] \epsilon_{\mu}^a(k) \epsilon_{\nu}^b(p) \epsilon_{\rho}(q). \quad (10)$$

Further below, a conversion of the neutral with respect to the the color orientation \hat{n} gluons is considered. Calculation of the Dirac trace and integration over variables x_{\parallel} , x_{\perp} , y_{\parallel} , y_{\perp} leads to

$$M = M^{(I)} + M^{(II)} = i(2\pi)^4 \delta^{(4)}(p + k - q) g^2 e \sum_l \mathcal{F}_{\mu\nu\rho}^l(p, k) F_l(p, k) \delta^{a8} \delta^{b8} \epsilon_{\mu}^a(k) \epsilon_{\nu}^b(p) \epsilon_{\rho}(q), \quad (11)$$

where tensors \mathcal{F}^l are composed of the $\delta_{\alpha\beta}$, momenta p_{α} , k_{α} and the tensor $f_{\alpha\beta}$. Form factors F_l have the structure

$$F_l(p, k) = \sum_f q_f \text{Tr}_{\hat{n}} \int_0^{\infty} ds_1 ds_2 ds_3 \left[\psi_l^{(I)}(s_1, s_2, s_3 | \hat{n}, m_f) + \psi_l^{(II)}(s_1, s_2, s_3 | \hat{n}, m_f) \right] \\ \times \exp \left\{ -p_{\parallel}^2 \phi_1(s_1, s_2, s_3) - p_{\parallel} k_{\parallel} \phi_2(s_1, s_2, s_3) - k_{\parallel}^2 \phi_3(s_1, s_2, s_3) \right. \\ \left. - p_{\perp}^2 \phi_4(s_1, s_2, s_3) - p_{\perp} k_{\perp} \phi_5(s_1, s_2, s_3) - k_{\perp}^2 \phi_6(s_1, s_2, s_3) - m_f^2 (s_1 + s_2 + s_3) \right\}, \quad (12)$$

where $\psi_l^{(I/II)}$ are functions of s_i , and the functions ϕ_1, \dots, ϕ_6 in (12) read

$$\begin{aligned}\phi_1 &= \frac{t_1(t_2 + t_3)}{t_1 + t_2 + t_3}, \quad \phi_2 = \frac{2t_1t_2}{t_1 + t_2 + t_3}, \quad \phi_3 = \frac{t_2(t_1 + t_3)}{t_1 + t_2 + t_3}, \\ \phi_4 &= \frac{\xi_1(\xi_2 + \xi_3)}{\xi_1 + \xi_2 + \xi_3 + \xi_1\xi_2\xi_3}, \quad \phi_5 = \frac{2\xi_1\xi_2}{\xi_1 + \xi_2 + \xi_3 + \xi_1\xi_2\xi_3}, \quad \phi_6 = \frac{\xi_2(\xi_1 + \xi_3)}{\xi_1 + \xi_2 + \xi_3 + \xi_1\xi_2\xi_3}, \\ t_j &= B|\hat{n}|s_j, \quad \xi_j = \frac{2t_j}{t_j \coth(t_j) + 1}.\end{aligned}\tag{13}$$

Full expressions for amplitude M (11) and form factors (12) are given in the Appendix. Some form factors in Euclidean kinematics are shown in Fig.2.

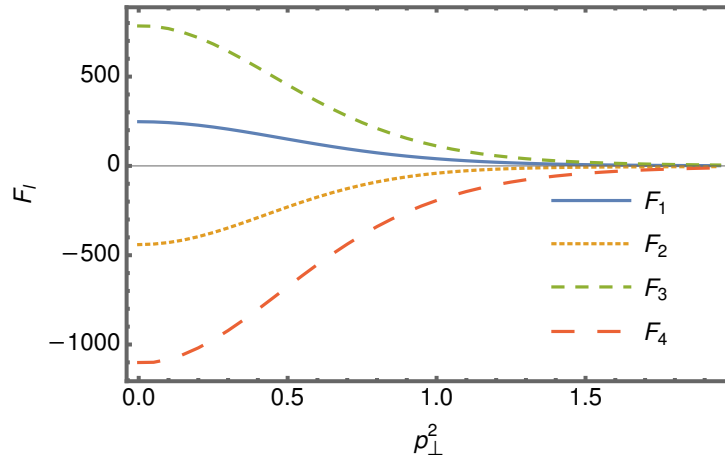


FIG. 2. Some of the form factors (12) as the functions of transverse gluon momenta $p_{\perp}^2 = k_{\perp}^2$ for longitudinal momenta $p_{\parallel}^2 = k_{\parallel}^2 = 1$. Dimensionless notation $p^2 = p^2/B$, $k^2 = k^2/B$ is used, form factors F_l are dimensionless. See Appendix for detailed form of F_l .

To calculate the on-shell amplitude squared $T = |M|^2$ one has to continue representation (12) to Minkowsky kinematics of the gluon and photon momenta:

$$p_{\parallel}^2 \rightarrow -p_{\parallel}^2, \quad k_{\parallel}^2 \rightarrow -k_{\parallel}^2, \quad p_{\parallel}k_{\parallel} \rightarrow -p_{\parallel}k_{\parallel}.\tag{14}$$

In Minkowski space-time, on-shell conditions for gluons and photon $p^2 = 0$, $(p+k)^2 = 0$ and $k^2 = 0$ impose the following relations

$$p_{\parallel}^2 = p_{\perp}^2, \quad k_{\parallel}^2 = k_{\perp}^2, \quad p_{\parallel}k_{\parallel} = p_{\perp}k_{\perp}\tag{15}$$

and the exponential phase factor $ip_{\perp}^{\mu}f_{\mu\nu}k_{\perp}^{\nu}$ vanishes since vectors p_{\perp} and k_{\perp} are parallel to each other.

The probability of photon production is given by the squared amplitude averaged over the initial gluon polarization states and summed over the final polarizations of photon

$$\bar{T}(p, k, q) = \Delta v \Delta \tau (2\pi)^4 \delta^4(p + k - q) T(p, k) ,$$

here $\Delta v \Delta \tau$ - is a space-time volume,

$$\begin{aligned} T(p, k) = & \frac{2\alpha\alpha_s^2}{\pi} \int_0^\infty ds_1 ds_2 ds_3 dr_1 dr_2 dr_3 F(s_1, s_2, s_3, r_1, r_2, r_3 | p, k) \\ & \times \exp \{ p_\perp^2 \Phi_1(s_1, s_2, s_3, r_1, r_2, r_3) + p_\perp k_\perp \Phi_2(s_1, s_2, s_3, r_1, r_2, r_3) + \\ & k_\perp^2 \Phi_3(s_1, s_2, s_3, r_1, r_2, r_3) - m_f^2 (s_1 + s_2 + s_3 + r_1 + r_2 + r_3) \} , \end{aligned} \quad (16)$$

where α and α_s - electromagnetic and strong coupling constants, and

$$\begin{aligned} \Phi_1 &= \phi_1(s_1, s_2, s_3) + \phi_1(r_1, r_2, r_3) - \phi_4(s_1, s_2, s_3) - \phi_4(r_1, r_2, r_3), \\ \Phi_2 &= \phi_2(s_1, s_2, s_3) + \phi_2(r_1, r_2, r_3) - \phi_5(s_1, s_2, s_3) - \phi_5(r_1, r_2, r_3), \\ \Phi_3 &= \phi_3(s_1, s_2, s_3) + \phi_3(r_1, r_2, r_3) - \phi_6(s_1, s_2, s_3) - \phi_6(r_1, r_2, r_3). \end{aligned} \quad (17)$$

Pre-exponential factor F is a polynomial in $p_\perp^2, k_\perp^2, k_\perp p_\perp$ with coefficients being the rational functions of proper times (s_j, r_j) and their combinations $(\xi_j(s_j), \xi_j(r_j))$ given in (13).

Since functions Φ_j are positive in the whole region of integration and grow linearly for $s_j \rightarrow \infty$, the proper time integrals in Eq. (16) converge only for the limited range of momenta p_\perp and k_\perp . For the case $k_\perp^2 = p_\perp^2$ the integral is coversges if

$$p_\perp^2 < \frac{3}{2} m_f^2, \quad (18)$$

as it can be seen from Eqs. (13) and (17).

A relevant analysis of the properties of the triangle diagram in the context of the photon splitting in the external electromagnetic field can be found in [43], as well as in [20, 21, 44, 45] for simpler case of two-point vacuum polarization in external magnetic field. Though a general prescription for analytical continuation of representation (16) to the arbitrary values of momenta in the complex plane has been formulated long time ago, its practical application is rather complicated.

The main purpose of the present paper is to indicate an impact of the vacuum long-range chromomagnetic field on the photon generation in deconfinement phase during the relativistic heavy ion collisions, and for that purpose it is sufficient to switch to the limit of strong field and small quark masses. In the massless quark limit the process of two gluon

conversion to a photon in the presence of long-range magnetic field was studied in [19] with the following result for the amplitude squared (the case of a single flavour) accounting for the lowest Landau levels (LLL) and first excited Landau level (1LL) for the quark propagator:

$$T(p, k) = \frac{2\alpha\alpha_s^2}{\pi} q_f^2 (2p_\perp^2 + k_\perp^2 + p_\perp k_\perp) \exp \left\{ -\frac{1}{|q_f B_{el}|} (p_\perp^2 + k_\perp^2 + p_\perp k_\perp) \right\}, \quad (19)$$

where B_{el} - is the strength of magnetic field.

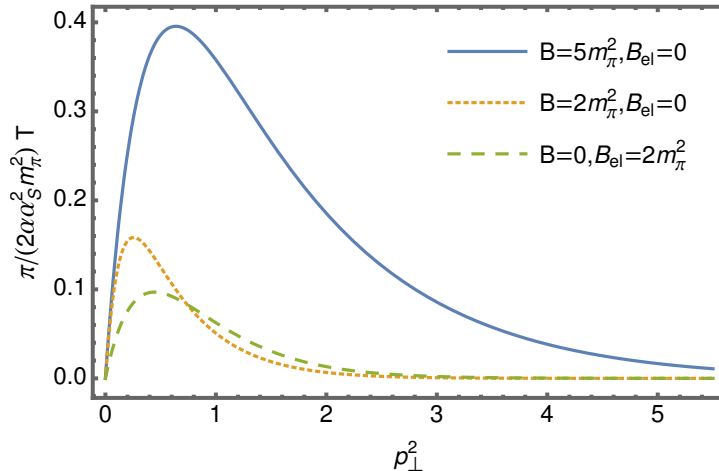


FIG. 3. Dependence of $T(p, k)$ on the gluon momenta for $k_\perp^2 = p_\perp^2$. The dashed line corresponds to the purely magnetic field B_{el} , dotted and solid lines represent the case of pure chromomagnetic field B with different strength (20). The contribution of u -quark is taken into account and the mass of the pion m_π is chosen as the scale. Dimensionless notation $p_\perp^2 = p_\perp^2/B$ is used.

Equation (19) can be easily generalized to the case of the presence of both magnetic and chromomagnetic fields by the replacement $|q_f B_{el}| \rightarrow |q_f B_{el} + \hat{n}B|$ with the result

$$T = \frac{2\alpha\alpha_s^2}{N_c\pi} q_f^2 \text{Tr}_{\hat{n}} (2p_\perp^2 + k_\perp^2 + p_\perp k_\perp) \exp \left\{ -\frac{p_\perp^2 + k_\perp^2 + p_\perp k_\perp}{|q_f B_{el} + \hat{n}B|} \right\}, \quad (20)$$

where the angle between magnetic and chromomagnetic fields is assumed to be zero, which corresponds to a minimum of the one-loop quark contribution to the free energy density [8].

As it is seen from the comparison of dotted and dashed lines in Fig.3, the chromomagnetic field enhances the photon production amplitude at small p_\perp in comparison with the effect of pure magnetic field with the same strength as the chromomagnetic one. One may expect that chromomagnetic field should be much stronger than the magnetic one, since the strength of the chromomagnetic field squared is of order of the value of the scalar gluon condensate. If so

than the effect of chromomagnetic field can be strong over a wide range of gluon momenta, see solid line in Fig.3. Since the magnetic field strength B_{el} decreases soon after the heavy ion collisions but the chromomagnetic field strength B is expected to be constant in the deconfined phase, then at a certain moment the production of photons will be determined only by the presence of the chromomagnetic field, see Fig.4.

The response of the invariant photon momentum distribution (25) is shown in Fig.6 at different magnetic field strength B_{el} , but at a fixed background chromomagnetic field strength B . It is clearly seen that a decrease in the magnetic field strength leads to a decrease in the level of the photon production signal and is further determined only by the strength of the chromomagnetic field.

Using relations

$$\begin{aligned} p^\mu &= (\omega_p/\omega_q)q^\mu, \\ k^\mu &= (\omega_k/\omega_q)q^\mu, \end{aligned} \tag{21}$$

one can rewrite (20) in the form

$$T(\omega_p, \omega_k) = \frac{2\alpha\alpha_s^2 q_\perp^2}{N_c \pi \omega_q^2} q_f^2 \text{Tr}_{\hat{n}} (2\omega_p^2 + \omega_k^2 + \omega_p \omega_k) \exp \left\{ -\frac{(\omega_p^2 + \omega_k^2 + \omega_p \omega_k) q_\perp^2}{|q_f B_{\text{el}} + \hat{n} B| \omega_q^2} \right\} \tag{22}$$

The invariant photon momentum distribution is thus given by

$$\omega_q \frac{dN}{d^3q} = \frac{\Delta v \Delta \tau}{2(2\pi)^3} \int \frac{d^3p}{(2\pi)^3 2\omega_p} \int \frac{d^3k}{(2\pi)^3 2\omega_k} n(\omega_p) n(\omega_k) \delta^4(q - k - p) T(\omega_p, \omega_k), \tag{23}$$

where $n(\omega)$ represents the distribution of gluons. Following the argumentation of the paper [19] we shall use the distribution

$$n(\omega) = \frac{\eta}{e^{\omega/\Lambda_s} - 1}, \tag{24}$$

where η represents the high gluon occupation factor. The factor $\Delta v \Delta \tau$ comes from squaring the delta function for energy-momentum conservation in amplitude. This factor represents the space-time volume where the reaction takes place and consists of the product of the spatial volume of the nuclear overlap region $\Delta v(t)$ at time t and the time interval $\Delta \tau$ where the magnetic and chromomagnetic fields can be taken as having a constant strength.

Finally, the invariant photon momentum distribution in the presence of chromomagnetic

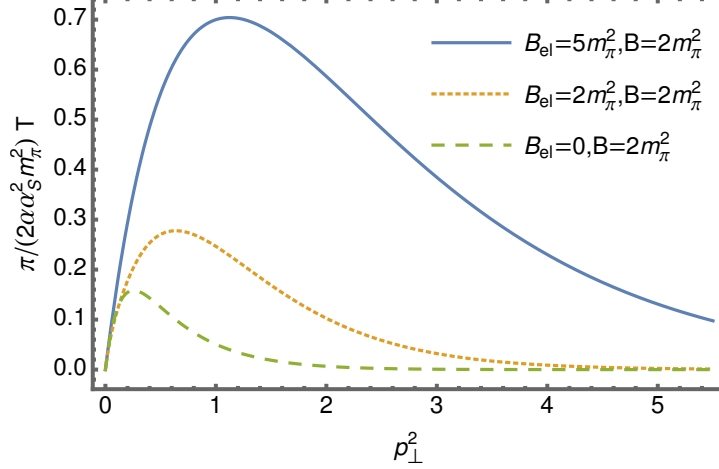


FIG. 4. Dependence (20) on the strength of magnetic field B_{el} in regime $p_{\perp}^2 = k_{\perp}^2$. The dashed curve corresponds only chromomagnetic field $B = 2m_{\pi}^2$ and the dotted and solid curves is the both presence fields with different magnetic field strength $B_{el} = 2m_{\pi}^2, B_{el} = 5m_{\pi}^2$ respectively. The contribution of only u -quark is taken into account. Dimensionless notation $p_{\perp} = p_{\perp}^2/B$ is used.

and magnetic fields can be represented in the form [19]

$$\frac{1}{2\pi\omega_q} \frac{dN}{d\omega_q} = \nu \Delta \tau \frac{\alpha \alpha_s^2 \pi}{2N_c (2\pi)^6 \omega_q} q_f^2 \text{Tr}_{\hat{n}} \int_0^{\omega_q} d\omega_p (2\omega_p^2 + \omega_q^2 - \omega_p \omega_q) e^{-g_f^B(\omega_p, \omega_q)} [I_0(g_f^B(\omega_p, \omega_q)) - I_1(g_f^B(\omega_p, \omega_q))] (n(\omega_p) n(|\omega_q - \omega_p|)), \quad (25)$$

where

$$g_f^B(\omega_p, \omega_q) = \frac{\omega_p^2 + \omega_q^2 - \omega_p \omega_q}{2|\hat{n}B + q_f B_{el}|}.$$

and $I_0(g_f(\omega_p, \omega_q)), I_1(g_f(\omega_p, \omega_q))$ - are the modified Bessel function of the first kind.

A comparison of the differential energy distribution of generated photons in the background magnetic field B_{el} and chromomagnetic field B is shown in Fig.5. Note that the integral in (25) is regularized at the lower limit using the infrared scale $\Lambda_{IR} = 0.05$ GeV which corresponds to thermal gluon distribution and was taken from the paper [46].

The response of the invariant photon momentum distribution (25) to a change in the magnetic field strength is shown in Fig.6, where magnetic field strength B_{el} varies, but the chromomagnetic field strength B stay unchanged. It is clearly seen that a decrease in the magnetic field strength leads to a decrease in the level of the photon production signal and is further determined by the strength of the chromomagnetic field. Thus the photon production occurs as long as the deconfined phase exists irrespective to the disappearance

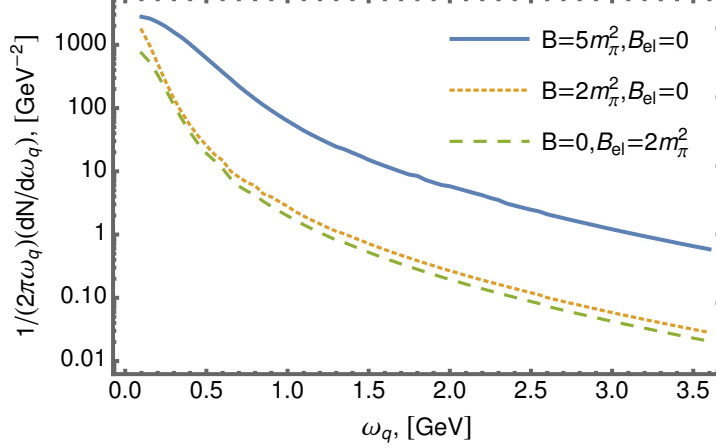


FIG. 5. Differential energy distribution of the generated photons for a pure magnetic field B_{el} (dashed line) and pure chromomagnetic field B (the dotted and solid curves). The contribution of only u -quark is taken into account and the pion mass $m_\pi = 0.135$ GeV is chosen as the scale. The factor $\Delta v \Delta \tau \alpha_s^2 / (2N_c (2\pi)^6) = 1 \text{GeV}^{-4}$.

of the initial magnetic field. As a matter of fact, the main role of magnetic field is to trigger the anisotropy of chromomagnetic field, which than stays as long as the deconfined phase exists.

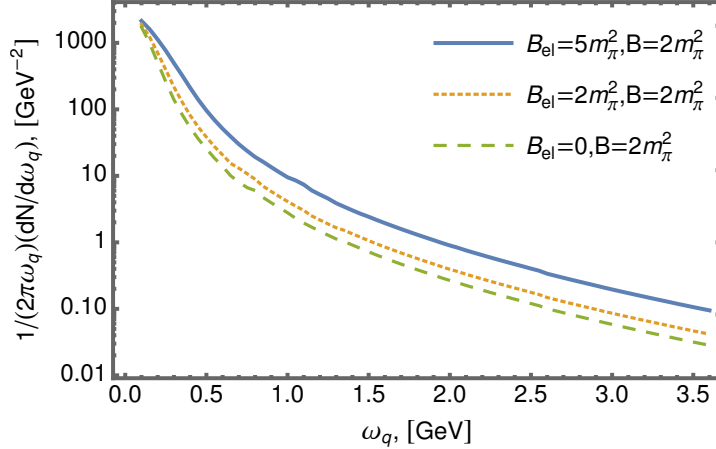


FIG. 6. Differential energy distribution of the generated photons. The dashed curve corresponds only chromomagnetic field $B = 2m_\pi^2$ and the dotted and solid curves is the both presence fields with different magnetic field strength $B_{el} = 2m_\pi^2, B_{el} = 5m_\pi^2$ respectively. The contribution of only u -quark is taken into account. The factor $\nu \Delta \tau \alpha_s^2 / (2N_c (2\pi)^6)$ is take to be equal to 1GeV^{-4} .

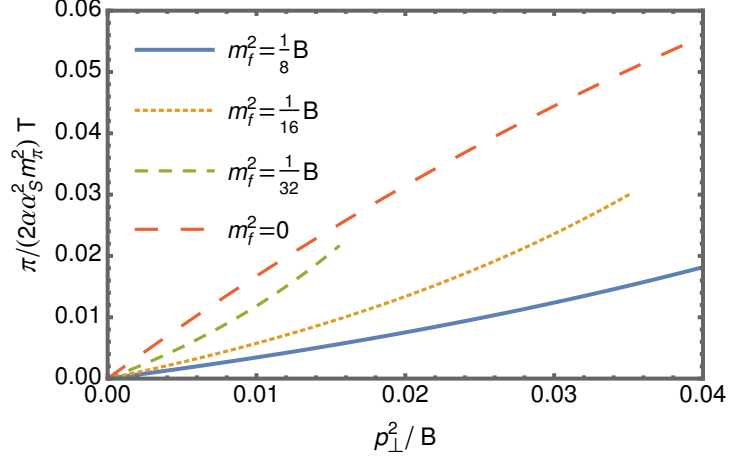


FIG. 7. The comparison of the amplitude square obtained by the Landau level decomposition for a massless quark (20) with the amplitude square (16) taking into account all Landau levels for different quark masses m_f at low gluon momenta in the regime $k_{\perp}^2 = p_{\perp}^2 < 3m_f^2/2$. The chromomagnetic field strength $B = 4m_{\pi}^2$ and magnetic field $B_{el} = 0$. Dimensionless notation $p_{\perp}^2 = p_{\perp}^2/B$ is used.

IV. DISCUSSION AND OUTLOOK

The estimates presented in this paper have illustrated at the qualitative level the plausibility of specific mechanism of photon generation in the quark-gluon plasma. In heavy ion collisions the conditions of Furry theorem are not satisfied due to the presence of strong anisotropic electromagnetic and chromomagnetic fields. Chromomagnetic field is likely to persists for a long time in comparison with a pure magnetic field [8, 9]. This mechanism is a kind of extension of the scenario intensively discussed in papers [6, 19]. Indeed, photon production in the process $gg \rightarrow \gamma$ may serve as a signal of the transition from the confinement to the deconfinement phase.

We have not attempted a comparison with available experimental data just for the reason that quantitative level of consideration requires, at least, taking into account nonzero quark masses, especially for the strange quark, and contribution of all Landau levels has to be accounted as well. Such a complete expression for amplitude of the process $gg \rightarrow \gamma$ is given in (11) and Appendix.

In order to estimate the deviation of the complete result from the the approximate sum of a couple of Landau levels and massless quarks, it makes sense to compute the amplitude

(11) in the interval $k_{\perp}^2 = p_{\perp}^2 < 3m_f^2/2$ and compare it with the approximate massless result. Such a comparison is given in Fig.7, which demonstrates an importance of contributions coming from the quarks with a mass of order of the current mass of the strange quark (solid line), as well as certain deviation of the light quark contribution (short dashed line) from the approximation (long dashed line).

As it has already been mentioned, obtained proper time integral representation is not appropriate for computation of photon distribution in the whole physically interesting interval of photon momentum. The analytical continuation of this representation to arbitrary momenta is under consideration and will be presented elsewhere.

ACKNOWLEDGMENTS

We are grateful to Vladimir Voronin for numerous useful discussions and valuable comments.

V. APPENDIX

The amplitude (11) consists of 32 terms. Below an explicit form of the tensor structures and corresponding form factors are listed.

Set of tensors $\mathcal{F}_{\mu\nu\rho}^l(p, k)$ includes

$$\begin{aligned}
\mathcal{F}_{\mu\nu\rho}^1(p, k) &= f_{\alpha\mu}f_{\beta\nu}f_{\lambda\rho}p_{\perp}^{\alpha}p_{\perp}^{\beta}p_{\perp}^{\lambda}, \quad \mathcal{F}_{\mu\nu\rho}^2(p, k) = f_{\alpha\mu}f_{\beta\nu}f_{\lambda\rho}p_{\perp}^{\alpha}p_{\perp}^{\beta}k_{\perp}^{\lambda}, \quad \mathcal{F}_{\mu\nu\rho}^3(p, k) = f_{\alpha\mu}f_{\beta\rho}f_{\lambda\nu}p_{\perp}^{\alpha}p_{\perp}^{\beta}k_{\perp}^{\lambda} \\
\mathcal{F}_{\mu\nu\rho}^4(p, k) &= f_{\alpha\mu}f_{\beta\nu}f_{\lambda\rho}p_{\perp}^{\alpha}k_{\perp}^{\beta}k_{\perp}^{\lambda}, \quad \mathcal{F}_{\mu\nu\rho}^5(p, k) = f_{\alpha\nu}f_{\beta\rho}f_{\lambda\mu}p_{\perp}^{\alpha}p_{\perp}^{\beta}k_{\perp}^{\lambda}, \quad \mathcal{F}_{\mu\nu\rho}^6(p, k) = f_{\alpha\nu}f_{\beta\mu}f_{\lambda\rho}p_{\perp}^{\alpha}k_{\perp}^{\beta}k_{\perp}^{\lambda}, \\
\mathcal{F}_{\mu\nu\rho}^7(p, k) &= f_{\alpha\rho}f_{\beta\mu}f_{\lambda\nu}p_{\perp}^{\alpha}k_{\perp}^{\beta}k_{\perp}^{\lambda}, \quad \mathcal{F}_{\mu\nu\rho}^8(p, k) = f_{\alpha\mu}f_{\beta\nu}f_{\lambda\rho}k_{\perp}^{\alpha}k_{\perp}^{\beta}k_{\perp}^{\lambda}, \\
\mathcal{F}_{\mu\nu\rho}^9(p, k) &= f_{\alpha\mu}p_{\perp}^{\alpha}\delta_{\nu\rho}p_{\perp}^2, \quad \mathcal{F}_{\mu\nu\rho}^{10}(p, k) = f_{\alpha\mu}p_{\perp}^{\alpha}\delta_{\nu\rho}p_{\perp}k_{\perp}, \quad \mathcal{F}_{\mu\nu\rho}^{11}(p, k) = f_{\alpha\mu}p_{\perp}^{\alpha}\delta_{\nu\rho}k_{\perp}^2, \\
\mathcal{F}_{\mu\nu\rho}^{12}(p, k) &= f_{\alpha\mu}p_{\perp}^{\alpha}\delta_{\nu\rho}^{\parallel}, \\
\mathcal{F}_{\mu\nu\rho}^{13}(p, k) &= f_{\alpha\nu}p_{\perp}^{\alpha}\delta_{\mu\rho}p_{\perp}^2, \quad \mathcal{F}_{\mu\nu\rho}^{14}(p, k) = f_{\alpha\nu}p_{\perp}^{\alpha}\delta_{\mu\rho}p_{\perp}k_{\perp}, \quad \mathcal{F}_{\mu\nu\rho}^{15}(p, k) = f_{\alpha\nu}p_{\perp}^{\alpha}\delta_{\mu\rho}k_{\perp}^2, \\
\mathcal{F}_{\mu\nu\rho}^{16}(p, k) &= f_{\alpha\nu}p_{\perp}^{\alpha}\delta_{\mu\rho}^{\parallel}, \\
\mathcal{F}_{\mu\nu\rho}^{17}(p, k) &= f_{\alpha\rho}p_{\perp}^{\alpha}\delta_{\mu\nu}p_{\perp}^2, \quad \mathcal{F}_{\mu\nu\rho}^{18}(p, k) = f_{\alpha\rho}p_{\perp}^{\alpha}\delta_{\mu\nu}p_{\perp}k_{\perp}, \quad \mathcal{F}_{\mu\nu\rho}^{19}(p, k) = f_{\alpha\rho}p_{\perp}^{\alpha}\delta_{\mu\nu}k_{\perp}^2, \\
\mathcal{F}_{\mu\nu\rho}^{20}(p, k) &= f_{\alpha\rho}p_{\perp}^{\alpha}\delta_{\mu\nu}^{\parallel}, \\
\mathcal{F}_{\mu\nu\rho}^{21}(p, k) &= f_{\alpha\mu}k_{\perp}^{\alpha}\delta_{\nu\rho}p_{\perp}^2, \quad \mathcal{F}_{\mu\nu\rho}^{22}(p, k) = f_{\alpha\mu}k_{\perp}^{\alpha}\delta_{\nu\rho}p_{\perp}k_{\perp}, \quad \mathcal{F}_{\mu\nu\rho}^{23}(p, k) = f_{\alpha\mu}k_{\perp}^{\alpha}\delta_{\nu\rho}k_{\perp}^2, \\
\mathcal{F}_{\mu\nu\rho}^{24}(p, k) &= f_{\alpha\mu}k_{\perp}^{\alpha}\delta_{\nu\rho}^{\parallel}, \\
\mathcal{F}_{\mu\nu\rho}^{25}(p, k) &= f_{\alpha\nu}k_{\perp}^{\alpha}\delta_{\mu\rho}p_{\perp}^2, \quad \mathcal{F}_{\mu\nu\rho}^{26}(p, k) = f_{\alpha\nu}k_{\perp}^{\alpha}\delta_{\mu\rho}p_{\perp}k_{\perp}, \quad \mathcal{F}_{\mu\nu\rho}^{27}(p, k) = f_{\alpha\nu}k_{\perp}^{\alpha}\delta_{\mu\rho}k_{\perp}^2 \\
\mathcal{F}_{\mu\nu\rho}^{28}(p, k) &= f_{\alpha\nu}k_{\perp}^{\alpha}\delta_{\mu\rho}^{\parallel}, \\
\mathcal{F}_{\mu\nu\rho}^{29}(p, k) &= f_{\alpha\rho}k_{\perp}^{\alpha}\delta_{\mu\nu}p_{\perp}^2, \quad \mathcal{F}_{\mu\nu\rho}^{30}(p, k) = f_{\alpha\rho}k_{\perp}^{\alpha}\delta_{\mu\nu}p_{\perp}k_{\perp}, \quad \mathcal{F}_{\mu\nu\rho}^{31}(p, k) = f_{\alpha\rho}k_{\perp}^{\alpha}\delta_{\mu\nu}k_{\perp}^2, \\
\mathcal{F}_{\mu\nu\rho}^{32}(p, k) &= f_{\alpha\rho}k_{\perp}^{\alpha}\delta_{\mu\nu}^{\parallel},
\end{aligned}$$

where $\delta_{\alpha\beta}^{\parallel} = \text{diag}(0, 0, 1, 1)$ - Kronecker symbol in the longitudinal space. Form factors $F^l(p, k)$ have the following representation

$$\begin{aligned}
F^l(p, k) &= \frac{2\sqrt{B}}{\pi} \sum_f q_f \text{Tr}_{\hat{n}} |\hat{n}|^3 \int_0^{\infty} \frac{ds_1 ds_2 ds_3}{(t_1 + t_2 + t_3)} \frac{\xi_1 \xi_2 \xi_3}{(\xi_1 + \xi_2 + \xi_3 + \xi_1 \xi_2 \xi_3)} \mathcal{P}^l(s_1, s_2, s_3) \\
&\quad \times \exp \left\{ -p_{\parallel}^2 \phi_1(s_1, s_2, s_3) - p_{\parallel} k_{\parallel} \phi_2(s_1, s_2, s_3) - k_{\parallel}^2 \phi_3(s_1, s_2, s_3) \right. \\
&\quad \left. - p_{\perp}^2 \phi_4(s_1, s_2, s_3) - p_{\perp} k_{\perp} \phi_5(s_1, s_2, s_3) - k_{\perp}^2 \phi_6(s_1, s_2, s_3) - m_f^2 (s_1 + s_2 + s_3) \right\},
\end{aligned}$$

$$t_j = B |\hat{n}| s_j, \quad \xi_j = \frac{2t_j}{t_j \coth(t_j) + 1}$$

$$\phi_1 = \frac{t_1(t_2 + t_3)}{t_1 + t_2 + t_3}, \quad \phi_2 = \frac{2t_1 t_2}{t_1 + t_2 + t_3}, \quad \phi_3 = \frac{t_2(t_1 + t_3)}{t_1 + t_2 + t_3},$$

$$\phi_4 = \frac{\xi_3(\xi_1 + \xi_2)}{\xi_1 + \xi_2 + \xi_3 + \xi_1 \xi_2 \xi_3}, \quad \phi_5 = \frac{2\xi_2 \xi_3}{\xi_1 + \xi_2 + \xi_3 + \xi_1 \xi_2 \xi_3}, \quad \phi_6 = \frac{\xi_2(\xi_1 + \xi_3)}{\xi_1 + \xi_2 + \xi_3 + \xi_1 \xi_2 \xi_3},$$

where $\mathcal{P}^l(s_1, s_2, s_3)$ - are the rational functions

$$\mathcal{P}^1(s_1, s_2, s_3) = \frac{32\xi_1^2 X [\coth(t_1)(C_{12} + 4) + 4D_{23}] [XY_{13}(Y_{23} + \xi_3) + Y_{13}^2 Y_{23} + X^2 \xi_3]}{Y_{13} (2Y + X)^3},$$

$$\mathcal{P}^2(s_1, s_2, s_3) = \left(16\xi_1 X [\coth(t_1)(C_{12} + 4) + 4D_{23}] \right. \\ \left. [X(2\xi_1 Y_{23} + \xi_3(Y_{23} + \xi_3)) + Y_{13}(\xi_1(Y_{23} + \xi_2) + \xi_3 Y_{23}) + X^2 \xi_3] \right) / (Y_{13}(Y + X)^3),$$

$$\mathcal{P}^3(s_1, s_2, s_3) = \left(8\xi_1 X \left[X \left(\coth(t_1) [2\xi_1(C_{23}\xi_2 + 4\xi_2 + \xi_3) + \right. \right. \right. \\ \left. \left. \xi_3(-2C_{23}\xi_2 - 7\xi_2 + 2\xi_3)] + D_{23} [2\xi_1(4\xi_2 + \xi_3) + \xi_3(2\xi_3 - 7\xi_2)] \right) + \right. \\ \left. Y_{13} \left(\coth(t_1) [\xi_1(2C_{23}\xi_2 + 8\xi_2 + \xi_3) - Y_{23}(2C_{23}\xi_2 + 8\xi_2 - \xi_3)] + \right. \right. \\ \left. \left. D_{23} [\xi_1(8\xi_2 + \xi_3) - 8\xi_2^2 - 7X_{23} + \xi_3^2] \right) + X^2 \xi_3 D \right] \right) / (Y_{13}(Y + X)^3),$$

$$\mathcal{P}^4(s_1, s_2, s_3) = - \left(8X\xi_2 \left[\left(\coth(t_1) [-2\xi_1^2(C_{23} + 4) + 2X_{12}(C_{23} + 4) - \right. \right. \right. \\ \left. \left. X_{13}(2C_{23} + 7) + \xi_3 Y_{23}] - D_{23} [8\xi_1^2 + \xi_1(7\xi_3 - 8\xi_2) - \xi_3 Y_{23}] \right) + \right. \\ \left. X \left(\coth(t_1) [\xi_3 - 2\xi_1(C_{23} + 4)] - D_{23} [8\xi_1 - \xi_3] \right) \right] \right) / ((Y + X)^3),$$

$$\mathcal{P}^5(s_1, s_2, s_3) = \left(8\xi_1 X \left[X \left(2 \coth(t_1) \xi_1 [\xi_2(C_{23} + 4) + \xi_3(2C_{23} + 7)] + \right. \right. \right. \\ \left. \left. \coth(t_1) \xi_3 [2\xi_3(2C_{23} + 7) - \xi_2] + D_{23} (8X_{12} + 14X_{13} - X_{23} + 14\xi_3^2) \right) + \right. \\ \left. Y_{13} \left(\coth(t_1) \xi_1 [2\xi_2(C_{23} + 4) + \xi_3(2C_{23} + 7)] - \right. \right. \\ \left. \left. \coth(t_1) Y_{23} [2\xi_2(C_{23} + 4) - \xi_3(2C_{23} + 7)] + D_{23} (8X_{12} + 7X_{13} - 8\xi_2^2 - X_{23} + 7\xi_3^2) \right) + \right. \\ \left. \left. X^2 \xi_3 [\coth(t_1) (2C_{23} + 7) + 7D_{23}] \right] \right) / (Y_{13}(Y + X)^3),$$

$$\mathcal{P}^6(s_1, s_2, s_3) = - \left(8X\xi_2 \left(\coth(t_1) [-2\xi_1^2(C_{23} + 4) + 2X_{12}(C_{23} + 4) + \right. \right. \\ \left. \left. \xi_3(2C_{23} + 7)Y_{23} - X_{13}] - D_{23} [8\xi_1^2 + \xi_1(\xi_3 - 8\xi_2) - 7\xi_3 Y_{23}] \right) + \right. \\ \left. X \left[-2 \coth(t_1) \xi_1 (C_{23} + 4) + \coth(t_1) \xi_3 (2C_{23} + 7) - D_{23} (8\xi_1 - 7\xi_3) \right] \right) / ((Y + X)^3),$$

$$\mathcal{P}^7(s_1, s_2, s_3) = -\frac{16X\xi_2[\coth(t_1)(C_{23} + 4) + 4D_{23}][\xi_1^2(Y_{23} + \xi_2) + \xi_3Y_{23} + X\xi_3]}{(Y + X)^3},$$

$$\mathcal{P}^8(s_1, s_2, s_3) = -\frac{32X\xi_2Y_{13}(\coth(t_1)(C_{23} + 4) + 4D_{23})}{(Y + X)^3},$$

$$\mathcal{P}^9(s_1, s_2, s_3) = -\frac{\xi_1[\coth(t_1)(C_{23} + 4) + 4D_{23}][XY_{13}(Y_{23} + \xi_3) + Y_{13}^2Y_{23} + X^2\xi_3]}{Y_{13}^2(Y + X)^3},$$

$$\mathcal{P}^{10}(s_1, s_2, s_3) = -\left(8X\xi_1(Y_{13} + X)[(\coth(t_1)[\xi_1(2C_{23}\xi_2 + 8\xi_2 + \xi_3) + \xi_3Y_{23}] + D_{23}[\xi_1(8\xi_2 + \xi_3) + \xi_3Y_{23}]) + X\xi_3Y\right) / (Y_{13}(Y + X)^3),$$

$$\begin{aligned} \mathcal{P}^{11}(s_1, s_2, s_3) = & \\ -\left(8X\xi_2[(\coth(t_1)[\xi_1^2(C_{23} + 4) + X_{13}(2C_{23} + 7) + \xi_3(C_{23} + 3)Y_{23}] + D_{23}[4\xi_1^2 + 7X_{13} + 3\xi_3Y_{23}]) + X(\coth(t_1)\xi_1(C_{23} + 4) + \coth(t_1)\xi_3(C_{23} + 3) + D_{23}(4\xi_1 + 3\xi_3))\right) & \\ & \Big/ ((Y + X)^3), \end{aligned}$$

$$\mathcal{P}^{12}(s_1, s_2, s_3) = \left(4X[Y_{13}[\coth(t_1)(\xi_1(4C_{23} + 15) - \xi_2 - \xi_3 + D_{23}(15\xi_1 - \xi_2 - \xi_3))] - X[\coth(t_1)(\xi_3 - \xi_1(4C_{23} + 15)) - D_{23}(15\xi_1 - \xi_3)]\right) / (Y_{13}(Y + X)^3),$$

$$\mathcal{P}^{13}(s_1, s_2, s_3) = -\frac{8X\xi_1[\coth(t_1)(C_{23} + 4) + 4D_{23}][XY_{13}(Y_{23} + \xi_3) + 4Y_{13}^2Y_{23} + 4X\xi_3]}{Y_{13}(Y + X)^3},$$

$$\mathcal{P}^{14}(s_1, s_2, s_3) = -\left(8X\xi_1(Y_{13} + X)(\coth(t_1)[2X_{12}(C_{23} + 4) + X_{13}(2C_{23} + 7) + \xi_3(2C_{23} + 7)Y_{23}] + D_{23}[\xi_1(8\xi_2 + 7\xi_3) + 7\xi_3Y_{23}] + X\xi_3[\coth(t_1)(2C_{23} + 7) + 7D_{23}])\right) / (Y_{13}(Y + X)^3),$$

$$\begin{aligned} \mathcal{P}^{15}(s_1, s_2, s_3) = & \\ -\left(8X\xi_2[(\coth(t_1)[\xi_1^2(C_{23} + 4) - \xi_3(C_{23} + 3)Y_{23} + X_{13}] + D_{23}[4\xi_1^2 + X_{13} - 3\xi_3Y_{23}]) + X(\coth(t_1)\xi_1(C_{23} + 4) - \coth(t_1)\xi_3(C_{23} + 3) + D_{23}(4\xi_1 - 3\xi_3))\right) & \\ & \Big/ ((Y + X)^3), \end{aligned}$$

$$\mathcal{P}^{16}(s_1, s_2, s_3) = \left(4X[Y_{13}[\coth(t_1)(\xi_1(2C_{23} + 9) - (2C_{23} + 7)Y_{23}) + D_{23}(9\xi_1 - 7Y_{23})] - X[-\coth(t_1)\xi_1(2C_{23} + 9) + \coth(t_1)\xi_3(2C_{23} + 7) - D_{23}(9\xi_1 - 7\xi_3)]\right) / (Y_{13}(Y + X)^3),$$

$$\mathcal{P}^{17}(s_1, s_2, s_3) = -\frac{8X\xi_1(4D_{23} + \coth(t_1)(4 + C_{23}))(X^2\xi_1 + Y_{13}^2Y_{23} + XY_{13}(Y_{23} + \xi_3))}{BY_{13}^2(X + Y)^3},$$

$$\mathcal{P}^{18}(s_1, s_2, s_3) = -\frac{16X\xi_2[\coth(t_1)(C_{23} + 4) + 4D_{23}][Y_{13}Y_{23} + X\xi_3]}{Y_{13}(Y + X)^3},$$

$$\mathcal{P}^{19}(s_1, s_2, s_3) = \frac{8X\xi_2(\coth(t_1)(C_{23} + 4) + 4D_{23})(\xi_1^2 + 2\xi_1Y_{23} + \xi_3Y_{23} + XY_{13})}{(Y + X)^3},$$

$$\mathcal{P}^{20}(s_1, s_2, s_3) = \frac{8(\coth(t_1)(C_{23} + 4) + 4D_{23})(Y_{13}(\xi_1 - Y_{23}) + X(\xi_1 - \xi_3))}{(Y_{13}(Y + X))^2},$$

$$\begin{aligned} \mathcal{P}^{21}(s_1, s_2, s_3) = & -\left(8X_{12}\xi_1[X\xi_3(\coth(t_1)(2\xi_1(C_{23}+3)+2C_{23}\xi_3-\xi_2+6\xi_3)+D_{23}(6\xi_1-\xi_2+6\xi_3))+\right. \\ & \left.\xi_3Y_{13}(\coth(t_1)(\xi_3(C_{23}+3)Y_{13}-\xi_2^2(C_{23}+4)-X_{23})-D_{23}(-3\xi_3Y_{13}+4\xi_2^2+X_{23}))+\right. \\ & \left.X^2\xi_3^2(\coth(t_1)(C_{23}+3)+3D_{23})\right) / (Y_{13}(Y+X)^3), \end{aligned}$$

$$\begin{aligned} \mathcal{P}^{22}(s_1, s_2, s_3) = & \left(8X\xi_2(\coth(t_1)[2X_{12}(C_{23}+4)+X_{13}(2C_{23}+7)+\xi_3(2C_{23}+7)Y_{23}]+ \right. \\ & \left. D_{23}[\xi_1(8\xi_2+7\xi_3)+7\xi_3Y_{23}]+X\xi_3[\coth(t_1)(2C_{23}+7)+7D_{23}])\right) / (Y_{13}(Y+X)^3), \end{aligned}$$

$$\mathcal{P}^{23}(s_1, s_2, s_3) = -\frac{1}{4}\mathcal{P}^8(s_1, s_2, s_3),$$

$$\begin{aligned} \mathcal{P}^{24}(s_1, s_2, s_3) = & \left(4X[\coth(t_1)(2C_{23}\xi_1-2C_{23}\xi_2+2C_{23}\xi_3+7\xi_1-9\xi_2+7\xi_3)+D_{23}(7\xi_1-9\xi_2+7\xi_3)+ \right. \\ & \left. X(\coth(t_1)(2C_{23}+7)+7D_{23})\right) / (Y+X)^2, \end{aligned}$$

$$\begin{aligned} \mathcal{P}^{25}(s_1, s_2, s_3) = & -\left(8X_{12}\xi_1[X\xi_3(\coth(t_1)(2\xi_1(C_{23}+3)+2C_{23}\xi_2+2C_{23}\xi_3+7\xi_2+6\xi_3)+ \right. \\ & \left. D_{23}(6\xi_1+7\xi_2+6\xi_3))+\xi_3Y_{13}(\coth(t_1)(\xi_3(C_{23}+3)Y_{13}+\xi_2^2(C_{23}+4)-X_{23}(2C_{23}+7))+ \right. \\ & \left. D_{23}(3\xi_3Y_{13}+4\xi_2^2+7X_{23}))+X^2\xi_3^2(\coth(t_1)(C_{23}+3)+3D_{23})\right) / (Y_{13}(Y+X)^3), \end{aligned}$$

$$\mathcal{P}^{26}(s_1, s_2, s_3) = \frac{8X(\coth(t_1)[\xi_1(2C_{23}\xi_2+8\xi_2+\xi_3)+\xi_3Y_{23}]+D_{23}[\xi_1(8\xi_2+\xi_3)+\xi_3Y_{23}]+X\xi_3D)}{(Y+X)^3},$$

$$\mathcal{P}^{27}(s_1, s_2, s_3) = -\frac{1}{4}\mathcal{P}^8(s_1, s_2, s_3),$$

$$\mathcal{P}^{28}(s_1, s_2, s_3) = \frac{4X(\coth(t_1)[-4C_{23}\xi_2 + \xi_1 - 15\xi_2 + \xi_3] + D_{23}[Y_{13} - 15\xi_2] + XD)}{(Y + X)^3},$$

$$\mathcal{P}^{29}(s_1, s_2, s_3) = -\frac{\xi_1[\coth(t_1)(C_{23} + 4) + 4D_{23}][XY_{13}Y_{23} + Y_{13}(\xi_1(Y_{23} + \xi_2) + Y_{23}^2) + X^2\xi_3]}{Y_{13}^2(Y + X)^3},$$

$$\mathcal{P}^{30}(s_1, s_2, s_3) = -\frac{16X\xi_1\xi_2[\coth(t_1)(C_{23} + 4) + 4D_{23}][Y_{13} + D]}{(Y + X)^3},$$

$$\mathcal{P}^{31}(s_1, s_2, s_3) = -\frac{1}{4}\mathcal{P}^8(s_1, s_2, s_3),$$

$$\mathcal{P}^{32}(s_1, s_2, s_3) = \frac{8X(\coth(t_1)(C_{23} + 4) + 4D_{23})(Y_{13} - \xi_2 + X)}{(Y + X)^3},$$

where the following notations is used

$$X = \xi_1\xi_2\xi_3, \quad X_{ij} = \xi_i\xi_j, \quad Y = \xi_1 + \xi_2 + \xi_3, \quad Y_{ij} = \xi_i + \xi_j,$$

$$C = \coth(t_1)\coth(t_2)\coth(t_3), \quad C_{ij} = \coth(t_i)\coth(t_j),$$

$$D = \coth(t_1) + \coth(t_2) + \coth(t_3), \quad D_{ij} = \coth(t_i) + \coth(t_j).$$

-
- [1] V. Skokov, A. Y. Illarionov, and V. Toneev, Estimate of the magnetic field strength in heavy-ion collisions, *Int. J. Mod. Phys. A* **24**, 5925 (2009), arXiv:0907.1396 [nucl-th].
- [2] V. Voronyuk, V. D. Toneev, W. Cassing, E. L. Bratkovskaya, V. P. Konchakovski, and S. A. Voloshin, (Electro-)Magnetic field evolution in relativistic heavy-ion collisions, *Phys. Rev. C* **83**, 054911 (2011), arXiv:1103.4239 [nucl-th].
- [3] A. Bzdak and V. Skokov, Anisotropy of photon production: initial eccentricity or magnetic field, *Phys. Rev. Lett.* **110**, 192301 (2013), arXiv:1208.5502 [hep-ph].
- [4] I. A. Shovkovy, Magnetic Catalysis: A Review, *Lect. Notes Phys.* **871**, 13 (2013), arXiv:1207.5081 [hep-ph].
- [5] K. Tuchin, Particle production in strong electromagnetic fields in relativistic heavy-ion collisions, *Adv. High Energy Phys.* **2013**, 490495 (2013), arXiv:1301.0099 [hep-ph].
- [6] A. Ayala, J. D. Castano-Yepes, C. A. Dominguez, L. A. Hernandez, S. Hernandez-Ortiz, and M. E. Tejeda-Yeomans, Prompt photon yield and elliptic flow from gluon fusion induced by magnetic fields in relativistic heavy-ion collisions, *Phys. Rev. D* **96**, 014023 (2017), [Erratum: *Phys.Rev.D* 96, 119901 (2017)], arXiv:1704.02433 [hep-ph].
- [7] M. D’Elia, L. Maio, F. Sanfilippo, and A. Stanzione, Phase diagram of qcd in a magnetic background, arXiv preprint arXiv:2111.11237 (2021).
- [8] B. V. Galilo and S. N. Nedelko, Impact of the strong electromagnetic field on the QCD effective potential for homogeneous Abelian gluon field configurations, *Phys. Rev. D* **84**, 094017 (2011), arXiv:1107.4737 [hep-ph].
- [9] S. N. Nedelko and V. E. Voronin, Domain wall network as QCD vacuum and the chromomagnetic trap formation under extreme conditions, *Eur. Phys. J. A* **51**, 45 (2015), arXiv:1403.0415 [hep-ph].
- [10] M. D’Elia, M. Mariti, and F. Negro, Susceptibility of the QCD vacuum to CP-odd electromagnetic background fields, *Phys. Rev. Lett.* **110**, 082002 (2013), arXiv:1209.0722 [hep-lat].
- [11] G. S. Bali, F. Bruckmann, G. Endrodi, F. Gruber, and A. Schaefer, Magnetic field-induced gluonic (inverse) catalysis and pressure (an)isotropy in QCD, *JHEP* **04**, 130, arXiv:1303.1328 [hep-lat].
- [12] M. D’Elia, L. Maio, F. Sanfilippo, and A. Stanzione, Confining and chiral properties of QCD

- in extremely strong magnetic fields, Phys. Rev. D **104**, 114512 (2021), arXiv:2109.07456 [hep-lat].
- [13] C. Bonati, M. D’Elia, M. Mariti, M. Mesiti, F. Negro, A. Rucci, and F. Sanfilippo, Magnetic field effects on the static quark potential at zero and finite temperature, Phys. Rev. D **94**, 094007 (2016), arXiv:1607.08160 [hep-lat].
- [14] K. Fukushima and J. M. Pawłowski, Magnetic catalysis in hot and dense quark matter and quantum fluctuations, Phys. Rev. D **86**, 076013 (2012), arXiv:1203.4330 [hep-ph].
- [15] S. Ozaki, QCD effective potential with strong $U(1)_{em}$ magnetic fields, Phys. Rev. D **89**, 054022 (2014), arXiv:1311.3137 [hep-ph].
- [16] H. Leutwyler, Constant Gauge Fields and their Quantum Fluctuations, Nucl. Phys. B **179**, 129 (1981).
- [17] S. N. Nedelko and V. E. Voronin, Energy-driven disorder in mean field QCD, Phys. Rev. D **103**, 114021 (2021), arXiv:2012.07081 [hep-ph].
- [18] C. Bonati, S. Cali, M. D’Elia, M. Mesiti, F. Negro, A. Rucci, and F. Sanfilippo, Effects of a strong magnetic field on the QCD flux tube, Phys. Rev. D **98**, 054501 (2018), arXiv:1807.01673 [hep-lat].
- [19] A. Ayala, J. D. Castaño Yepes, I. Dominguez Jimenez, J. Salinas San Martín, and M. E. Tejeda-Yeomans, Centrality dependence of photon yield and elliptic flow from gluon fusion and splitting induced by magnetic fields in relativistic heavy-ion collisions, Eur. Phys. J. A **56**, 53 (2020), arXiv:1904.02938 [hep-ph].
- [20] S. L. Adler, J. N. Bahcall, C. G. Callan, and M. N. Rosenbluth, Photon splitting in a strong magnetic field, Phys. Rev. Lett. **25**, 1061 (1970).
- [21] V. O. Papanyan and V. I. Ritus, Vacuum polarization and photon splitting in an intense field, Zh. Eksp. Teor. Fiz. **61**, 2231 (1971).
- [22] V. N. Baier, V. M. Katkov, and V. M. Strakhovenko, An Operator Approach to Quantum Electrodynamics in External Field. 2. Electron Loops, Zh. Eksp. Teor. Fiz. **68**, 405 (1975).
- [23] A. Adare *et al.* (PHENIX), Enhanced production of direct photons in Au+Au collisions at $\sqrt{s_{NN}} = 200$ GeV and implications for the initial temperature, Phys. Rev. Lett. **104**, 132301 (2010), arXiv:0804.4168 [nucl-ex].
- [24] A. Adare *et al.* (PHENIX), Observation of direct-photon collective flow in $\sqrt{s_{NN}} = 200$ GeV Au+Au collisions, Phys. Rev. Lett. **109**, 122302 (2012), arXiv:1105.4126 [nucl-ex].

- [25] J. Adam *et al.* (ALICE), Direct photon production in Pb-Pb collisions at $\sqrt{s_{NN}} = 2.76$ TeV, Phys. Lett. B **754**, 235 (2016), arXiv:1509.07324 [nucl-ex].
- [26] C. Shen, C. Park, J.-F. Paquet, G. S. Denicol, S. Jeon, and C. Gale, Direct photon production and jet energy-loss in small systems, Nucl. Phys. A **956**, 741 (2016), arXiv:1601.03070 [hep-ph].
- [27] J.-F. Paquet, C. Shen, G. S. Denicol, M. Luzum, B. Schenke, S. Jeon, and C. Gale, Production of photons in relativistic heavy-ion collisions, Phys. Rev. C **93**, 044906 (2016), arXiv:1509.06738 [hep-ph].
- [28] R. Chatterjee, D. K. Srivastava, U. W. Heinz, and C. Gale, Elliptic flow of thermal dileptons in relativistic nuclear collisions, Phys. Rev. C **75**, 054909 (2007), arXiv:nucl-th/0702039.
- [29] H. van Hees, C. Gale, and R. Rapp, Thermal Photons and Collective Flow at the Relativistic Heavy-Ion Collider, Phys. Rev. C **84**, 054906 (2011), arXiv:1108.2131 [hep-ph].
- [30] F.-M. Liu and S.-X. Liu, Quark-gluon plasma formation time and direct photons from heavy ion collisions, Phys. Rev. C **89**, 034906 (2014), arXiv:1212.6587 [nucl-th].
- [31] O. Linnyk, V. P. Konchakovski, W. Cassing, and E. L. Bratkovskaya, Photon elliptic flow in relativistic heavy-ion collisions: hadronic versus partonic sources, Phys. Rev. C **88**, 034904 (2013), arXiv:1304.7030 [nucl-th].
- [32] B. G. Zakharov, Phenomenology of collinear photon emission from quark-gluon plasma in AA collisions, JETP Lett. **106**, 283 (2017), arXiv:1707.08602 [nucl-th].
- [33] G. Vujanovic, J.-F. Paquet, S. Ryu, C. Shen, G. S. Denicol, S. Jeon, C. Gale, and U. Heinz, Bulk viscous effects on flow and dilepton radiation in a hybrid approach, Nucl. Phys. A **967**, 692 (2017), arXiv:1704.04687 [nucl-th].
- [34] V. V. Goloviznin, A. M. Snigirev, and G. M. Zinovjev, Towards azimuthal anisotropy of direct photons, JETP Lett. **98**, 61 (2013), arXiv:1209.2380 [hep-ph].
- [35] V. V. Goloviznin, A. V. Nikolskii, A. M. Snigirev, and G. M. Zinovjev, Probing confinement by direct photons and dileptons, Eur. Phys. J. A **55**, 142 (2019), arXiv:1804.00559 [hep-ph].
- [36] S. N. Nedelko and V. E. Voronin, Regge spectra of excited mesons, harmonic confinement and QCD vacuum structure, Phys. Rev. D **93**, 094010 (2016), arXiv:1603.01447 [hep-ph].
- [37] S. N. Nedelko and V. E. Voronin, Influence of confining gluon configurations on the $P \rightarrow \gamma^* \gamma$ transition form factors, Phys. Rev. D **95**, 074038 (2017), arXiv:1612.02621 [hep-ph].
- [38] M. Faber, H. Markum, S. Olejnik, and W. Sakuler, Topological charges and confinement in

- lattice QCD, Phys. Lett. B **334**, 145 (1994).
- [39] P. J. Moran and D. B. Leinweber, Buried treasure in the sand of the QCD vacuum, in *QCD Downunder II* (2008) arXiv:0805.4246 [hep-lat].
- [40] V. G. Bornyakov, E. M. Ilgenfritz, B. V. Martemyanov, V. K. Mitrjushkin, and M. Müller-Preussker, Topology across the finite temperature transition studied by overimproved cooling in gluodynamics and QCD, Phys. Rev. D **87**, 114508 (2013), arXiv:1304.0935 [hep-lat].
- [41] N. Y. Astrakhantsev, V. V. Braguta, A. Y. Kotov, D. D. Kuznedev, and A. A. Nikolaev, Lattice study of QCD at finite chiral density: topology and confinement, Eur. Phys. J. A **57**, 15 (2021), arXiv:1902.09325 [hep-lat].
- [42] M. P. Lombardo and A. Trunin, Topology and axions in QCD, Int. J. Mod. Phys. A **35**, 2030010 (2020), arXiv:2005.06547 [hep-lat].
- [43] V. O. Papanyan and V. I. Ritus, Three-photon interaction in an intense field and scaling invariance, Zh. Eksp. Teor. Fiz. **65**, 1756 (1973).
- [44] V.I.Ritus, Vacuum polarization and photon splitting in an intense field, Zh. Eksp. Teor. Fiz. **57**, 2176 (1969).
- [45] V. I. Ritus, Radiative corrections in quantum electrodynamics with intense field and their analytical properties, Annals Phys. **69**, 555 (1972).
- [46] L. McLerran and B. Schenke, The Glasma, Photons and the Implications of Anisotropy, Nucl. Phys. A **929**, 71 (2014), arXiv:1403.7462 [hep-ph].